Boundedness of Synchronverters using bounded integral control

George C. Konstantopoulos, Qing-Chang Zhong, Beibei Ren and Miroslav Krstic

Abstract— **Synchronverters are grid-friendly inverters that mimic the operation of conventional synchronous generators. In this paper, the non-linear stability of the synchronverter in the sense of boundedness is investigated and proven for the first time. To this end, initially, the complete non-linear model of the synchronverter is obtained and then the field-excitation current loop of the synchronverter is implemented using a bounded integral control (BIC) structure, as proposed by the authors in the literature. While maintaining the original synchronverter operation near the rated value, the BIC additionally guarantees that the field-excitation current will remain bounded in a given range. Using non-linear analysis and input-to-state stability theory, it is proven that the frequency dynamics will remain bounded which leads to a bounded synchronverter voltage and finally results in the stability of the closed-loop system in the sense of boundedness. Extensive simulation results verify that the proposed synchronverter with the BIC approximates the behavior of the original synchronverter near the rated value with a guaranteed bounded performance.**

I. Introduction

Nowadays, due to the rapid increase of renewable energy systems penetration to the electrical grid, distributed generation (DG) units play an important role in the power system operation. Their integration is achieved using suitably controlled dc to ac power electronic devices, also called inverters. Therefore, both the control design and the stability analysis of power electronic inverters connected to the grid have become major issues in both control and power research communities [1].

Since most of the conventional power plants are connected to the grid through synchronous generators (SG), several researchers have proposed control strategies for the inverters of the DGs to imitate some of the aspects of the operation of conventional SGs [1], [2], [3], [4]. In this frame, the real and the reactive power injected to the grid by the DG can be controlled using several droop control mechanisms [4], [5], [6]. Recently, the idea of operating the inverter in a grid-friendly manner in order to mimic the dynamic behavior of the SG was proposed. These types of inverters are called synchronverters [1], [7], [8]. Synchronverters introduce the same dynamic equations with a SG and actually operate as a SG with a small capacitor bank connected in parallel to the stator terminals. An important advantage of the synchronverter technology is that some of the system parameters, such as the inertia, the friction coefficient, the field and mutual inductance, can be suitably chosen in order to improve the dynamic performance. Synchronverters can be also used in a rectifier mode, thus making rectifier-fed loads to operate as synchronous motors [9]. Therefore, most of the power systems that are connected to the grid (power plants, DGs, loads) can operate in the same manner described by the synchronverter technology. This can significantly improve the behavior of the power network.

Although using the synchronverter technology to control the power inverters creates a universal way of operating all power systems, the stability of the synchronverter has not been proven yet. Since the synchronverter is often linked to the grid via an LCL filter, it is important to guarantee that the grid-connected system will remain stable at all times. However, this is not an easy task due to the non-linearities of the control design that arise from the calculation of the real and the reactive power. Small-signal analysis has been used to provide local stability results of grid connected inverters [10]. However, the non-linear dynamics of the closed-loop system make non-linear analysis essential to achieve global stability results. Recently, a non-linear control strategy with a power-damping property was proposed to guarantee non-linear system stability [11], while requiring knowledge of the filter parameters. As a result, according to the authors' knowledge, non-linear stability of the synchronverter system, which incorporates the advantages of the SG and acts independently from the system parameters, has not been solved yet.

In this paper, the non-linear stability in the sense of boundedness of the synchronverter connected to the grid using an LCL filter, as proposed in [1], [7], is investigated. The complete non-linear model of the system is firstly derived using the Kron-reduced network approach [12]. From the model structure, it is observed that closed-loop system stability is hard to investigate mainly due to the non-linearities caused by the calculation of the real and the reactive power. The non-linearities appear to both the frequency and the field-excitation current loop of the control part of the synchronverter. To this end, in this paper, the field-excitation current control is implemented using the bounded integral control (BIC) structure, as recently proposed by the authors [13]. The BIC guarantees that the field-excitation current will approximate the behavior of the original synchronverter near the rated value and additionally guarantee that it will stay within a given range. Based on this operation, the non-

The financial support from the EPSRC, UK under Grant No. EP/J01558X/1 is greatly appreciated.

G. C. Konstantopoulos and Q.-C. Zhong are with the Department of Automatic Control and Systems Engineering, The Univesity of Sheffield, Sheffield S1 3JD, U.K. g.konstantopoulos@sheffield.ac.uk, zhongqc@ieee.org

B. Ren is with the Department of Mechanical Engineering, Texas Tech University, Lubbock, TX 79409, USA. beibei.ren@ttu.edu

M. Krstic is with the Department of Mechanical and Aerospace Engineering, University of California, San Diego, 9500 Gilman Drive, La Jolla, CA 92093-0411, USA krstic@ucsd.edu

linear input-to-state stability theory is used to guarantee that the frequency loop is stable and the frequency will always remains bounded. As a result, the output voltage of the synchronverter is proven to remain bounded and guarantees non-linear closed-loop system stability in the sense of boundedness. Extensive simulation results are provided to compare the original synchronverter, as proposed in [1], [7], with the synchronverter operating with the BIC and to verify that the proposed approach can maintain the original synchronverter theory with guaranteed stability.

The paper is organised as follows. In Section II, a brief introduction of the bounded integral control is presented. In Section III, the complete non-linear dynamic model of the synchronverter is derived. In Section IV, the stability of the synchronverter in the sense of boundedness is investigated. First the BIC is used to implement the field-excitation current and guarantee a bounded response and then the frequency and consequently the synchronverter output voltage are proven to remain bounded. In Section V, simulation results are provided to compare the original synchronverter with the proposed synchronverter with BIC structure and finally, in Section VI, some conclusions are drawn.

II. Bounded integral control background

Integral control (IC) is widely used in control systems in order to achieve accurate regulation. However, when used in a closed-loop form, IC cannot guarantee stability at all times. To this end, a bounded integral controller (BIC) structure that approximates the behavior of the IC near steady-state and produces an output with a given bound has been recently proposed [13]. In this section, a brief introduction of the BIC is presented.

The traditional IC takes the form

$$u(t) = \int_0^t g\left(x(\tau)\right) d\tau \tag{1}$$

which introduces a dynamic controller that can be written as

$$\begin{aligned} u &= w && (2)\\ \dot{w} &= g(x), && (3) \end{aligned}$$

where $g(x)$ is the function to be regulated to zero.

The BIC, as proposed in [13], introduces a second controller state and is given in the following general form:

$$\begin{aligned} u &= w && (4)\\ \begin{bmatrix} \dot{w} \\ \dot{w}_q \end{bmatrix} &= A_c \begin{bmatrix} w \\ w_q \end{bmatrix} && (5) \end{aligned}$$

with $A_c =$

$$\begin{bmatrix} -k\left(\frac{w^2}{u_{max}^2}+\frac{(w_q-b)^2}{\epsilon^2}-1\right) & g(x)c \\ -\frac{\epsilon^2}{u_{max}^2}g(x)c & -k\left(\frac{w^2}{u_{max}^2}+\frac{(w_q-b)^2}{\epsilon^2}-1\right) \end{bmatrix}$$

where w and w_q are the controller state variables, b is a non-negative constant and u_{max}, k, ϵ, c are positive constants. Consider the following ellipse as the Lyapunov function candidate

$$V = \frac{w^2}{u_{max}^2} + \frac{w_q^2}{\epsilon^2}. \tag{6}$$

Its time derivative yields

$$\begin{aligned} \dot{V} &= \frac{2w\dot{w}}{u_{max}^2} + \frac{2w_q\dot{w}_q}{\epsilon^2} \\ &= -2k\left(\frac{w^2}{u_{max}^2}+\frac{(w_q-b)^2}{\epsilon^2}-1\right)\left(\frac{w^2}{u_{max}^2}+\frac{w_q^2}{\epsilon^2}\right) \\ &= -2k\left(\frac{w^2}{u_{max}^2}+\frac{(w_q-b)^2}{\epsilon^2}-1\right)V. \end{aligned} \tag{7}$$

This shows that the sign of $\dot{V}$ is related to another ellipse with center the point $(0, b)$ given by

$$C = \left\{ w, w_q \in R : \frac{w^2}{u_{max}^2} + \frac{(w_q-b)^2}{\epsilon^2} = 1 \right\} \tag{8}$$

and is positive inside C and negative outside. Therefore, there exists an ultimate bound for the controller states and as a result the states w and w_q are always bounded independently from the function $g(x)$ to be regulated.

Different operation modes could be introduced via selecting appropriate values for the parameters. If the controller output u is required to stay within a given bound, with the maximum absolute value given by u_{max}, then the rest of the controller parameters can be chosen as $b = 0$, $\epsilon = 1$, $k \geq 0$, and $c = \frac{w_q u_{max}^2}{u_{max}^2 - (u^*)^2}$ to adapt to the varying w_q. Here, u^* is the nominal value or the normal operating point of u. In this case, it has been proven that the controller states w and w_q are attracted onto and thereafter exclusively move on the ellipse

$$W_0 = \left\{ \forall w, w_q \in R \in \frac{w^2(t)}{u_{max}^2} + {w_q}^2(t) = 1 \right\} \tag{9}$$

with the angular velocity $\dot{\theta} = \frac{g(x)c}{u_{max}}$. This means that the controller output $u = w$ is always bounded in the interval $[-u_{max}, u_{max}]$ and since at the desired equilibrium $g(x) = 0$, then $\dot{\theta} = 0$ and the states stop moving and converge to the desired point $\left(u^*, w_q^*\right)$ on ellipse W_0. This is depicted in Fig. 1. It has been proven that the BIC recovers the IC at the steady state. Additionally, no undesired oscillations appear on the closed set W_0 and the controller states will always stay on the first two quadrants since $\dot{\theta} \to 0$ as $w \to \pm u_{max}$ due to the adaptive choice of the parameter c. Therefore, in any case, the controller output u remains as a bounded signal in the desired range $[-u_{max}, u_{max}]$ independently from the function $g(x)$.

III. Synchronverter model

Synchronverters are inverters that mimic the operation of a synchronous generator. The complete synchronverter dynamic model results by combining the power part and the control part [1], [7].

A. Power part

The power part of the synchronverter consists of a three-phase inverter connected to the grid through an LCL filter as shown in Fig. 2. Using the Kron-reduced network approach [12], the node of the capacitor bank can be eliminated and

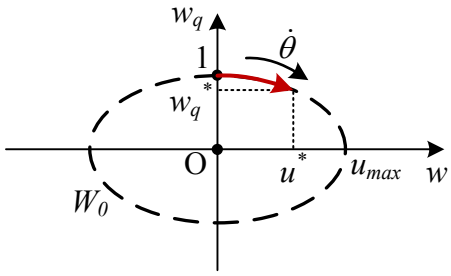

Fig. 1. The states phase portrait of BIC on the $w - w_q$ plane

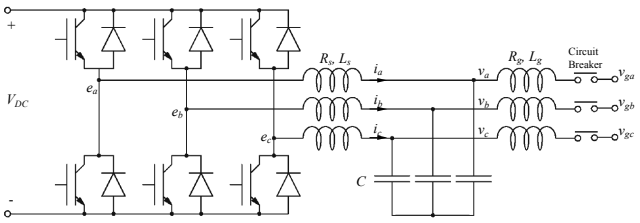

Fig. 2. The power part of a synchronverter

result in the per-phase system of the synchronverter connected to the grid as shown in Fig. 3. In this representation, the synchronverter and the grid are connected via a complex admittance $Y = G+jB$ with conductance G and susceptance B, while G_s, G_g and B_s, B_g are the shunt conductance and susceptance of the SV and the grid respectively.

Thus the real and reactive power at the output of the synchronverter are given as

$$P_s = 3\left(G_s + G\right)E^2 - 3EV_g\left(G\cos\delta + B\sin\delta\right) \quad (10)$$

$$Q_s = -3\left(B_s + B\right)E^2 + 3EV_g\left(G\sin\delta - B\cos\delta\right) \quad (11)$$

where E and V_g are the RMS phase voltage of the synchronverter and the grid, respectively, and $\delta = \theta - \theta_g$ is the phase difference between e and v_g, as shown in Fig. 3.

B. Control part

The control part of the synchronverter consists of a frequency $\omega = \dot{\theta}$ loop and a field-excitation current i_f loop as shown in Fig. 4. The dynamics of the synchronverter frequency ω are given by

$$\begin{aligned}\dot{\omega} &= \frac{1}{J}\left(T_m - T_e\right) - \frac{D_p}{J}\left(\omega - \omega_r\right) \\ &= \frac{1}{J}\left(T_m - \frac{P_s}{\omega}\right) - \frac{D_p}{J}\left(\omega - \omega_g\right) \end{aligned} \quad (12)$$

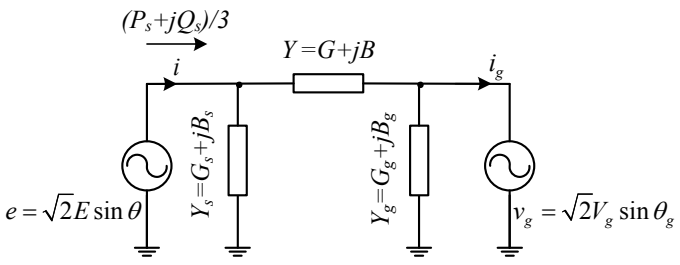

Fig. 3. Per-phase equivalent diagram using Kron-reduced network approach

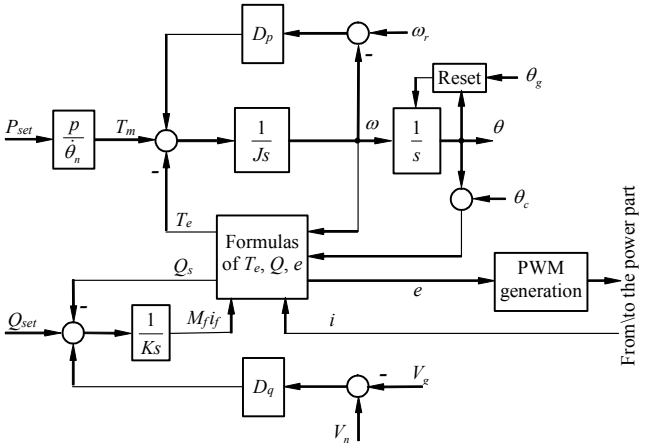

Fig. 4. The control part of a synchronverter

where T_e is the electromagnetic torque, i.e. $P_s = T_e\omega$ and T_m is the mechanical torque defined from the desired real output power $P_{set} = T_m\omega_n$, where ω_n is the rated frequency. ω_r is either equal to the grid frequency ω_g or to the rated frequency ω_n when the frequency droop is disabled or enabled, respectively, J is the imaginary moment of inertia and D_p is the frequency droop coefficient, with J and D_p being positive constants.

The dynamics of the field-excitation current i_f are given from the expression

$$\dot{i}_f = \frac{1}{KM_f}\left(Q_{set} - Q_s\right) + \frac{D_q}{KM_f}\left(V_n - V_g\right) \quad (13)$$

where Q_{set} is the desired reactive output power, V_n is the RMS rated voltage, M_f is the maximum mutual inductance between the stator windings and the field winding, D_q is the voltage droop coefficient and is non-negative and K is a positive constant gain.

The electromagnetic torque T_e is defined as

$$T_e = M_f i_f \left\langle i, \widetilde{\sin}\theta \right\rangle \quad (14)$$

where i is the inverter output current and the reactive power Q_s is given in the terms of the synchronverter parameters as

$$Q_s = -\omega M_f i_f \left\langle i, \widetilde{\cos}\theta \right\rangle \quad (15)$$

where $\langle\cdot,\cdot\rangle$ denotes the conventional inner product and

$$\widetilde{\sin}\theta = \begin{bmatrix} \sin\theta \\ \sin\left(\theta - \frac{2\pi}{3}\right) \\ \sin\left(\theta + \frac{2\pi}{3}\right) \end{bmatrix}, \quad \widetilde{\cos}\theta = \begin{bmatrix} \cos\theta \\ \cos\left(\theta - \frac{2\pi}{3}\right) \\ \cos\left(\theta + \frac{2\pi}{3}\right) \end{bmatrix}.$$

The synchronverter output voltage is then given by

$$e = \omega M_f i_f \widetilde{\sin}\theta \quad (16)$$

which implies that the RMS synchronverter output voltage is

$$E = \frac{\omega M_f i_f}{\sqrt{2}}. \quad (17)$$

C. Complete Synchronverter model

The complete dynamic model of the synchronverter is obtained from equations (12) and (13) combined with (10), (11) and (17). It should be noted that in order to guarantee the stability of a synchronverter connected to the grid in the sense of boundedness, the frequency ω and the field-excitation current i_f should be proven to remain bounded. If ω and i_f are bounded, then from (17), the RMS output voltage E is bounded and taking into account that the grid voltage V_g and frequency ω_g are bounded signals (infinite bus), then P_s, Q_s, P_g and Q_g will remain bounded. The difficulty of proving system stability lies in the non-linear dynamics of the system arising from the non-linear expressions of P_s and Q_s. This problem can be dealt with the bounded integral control structure for obtaining the field-excitation current i_f as described in the sequel.

IV. Boundedness of synchronverters

A. Boundedness of the field-excitation current i_f using the BIC

When the synchronverter is connected to the grid, the RMS output voltage should be maintained within a range from the rated voltage V_n, often according to the technical requirements of the synchronverter. Usually a percentage $p \cdot 100\%$ over and below the rated voltage V_n is assumed to give a maximum bound for the voltage $E_{max} = (1+p)V_n$ to avoid over-voltage phenomena and a minimum bound $E_{min} = (1-p)V_n$ to avoid under-voltage phenomena which could lead to high currents flowing from the grid. Then from (17), the condition

$$(1-p)V_n \leq \frac{\omega M_f i_f}{\sqrt{2}} \leq (1+p)V_n$$

should hold. If it is assumed that the frequency ω is regulated closely to the rated frequency ω_n (which is normally the case), the corresponding maximum and minimum bound for the field-excitation current i_f can be calculated as

$$\frac{(1-p)V_n\sqrt{2}}{\omega_n M_f} \leq i_f \leq \frac{(1+p)V_n\sqrt{2}}{\omega_n M_f}. \tag{18}$$

Since the nominal value of the field-excitation current i_f is $i_{fn} = \frac{V_n\sqrt{2}}{\omega_n M_f}$, there is

$$|i_f - i_{fn}| \leq \Delta i_{fmax}, \tag{19}$$

where $\Delta i_{fmax} = \frac{pV_n\sqrt{2}}{\omega_n M_f}$, according to (18). This can be achieved by using the BIC as presented in Section II to replace the integrator (13). Because of the shift of i_f by i_{fn} in (19), there is a need to shift the center of the ellipse W_0 from the origin to $(i_{fn}, 0)$ on the $i_f - i_{fq}$ plane. This results in the bounded integral controller for the field-excitation current i_f given in eq. (20), which is obtained from (5) with $b = 0$, $\epsilon = 1$, $k \geq 0$ and $c = i_{fq}$.

Note that since i_f and i_{fq} will operate on the ellipse

$$W_0 = \left\{ \forall i_f, i_{fq} \in R \in \frac{(i_f - i_{fn})^2}{\Delta i_{fmax}^2} + {i_{fq}}^2 = 1 \right\},$$

then near the rated value, i.e. when i_f is near i_{fn}, the first equation of (20) becomes

$$\dot{i}_f \approx \frac{1}{KM_f}(Q_{set} - Q_s) + \frac{D_q}{KM_f}(V_n - V_g) \tag{21}$$

since $i_{fq} \approx 1$, which proves that the proposed BIC for the field excitation current i_f will approximate the original synchronverter current response (13) near the rated value. Additionally, it is also guaranteed from the BIC operation that $|i_f - i_{fn}| \leq \Delta i_{fmax}$ will hold true independently from the function $\frac{1}{KM_f}(Q_{set} - Q_s) + \frac{D_q}{KM_f}(V_n - V_g)$ that needs to be regulated at zero. This is a crucial property for guaranteeing the system stability in the sense of boundedness, as shown in the following subsection.

B. Boundedness of the synchronverter frequency and voltage

As it is proven in the previous section, based on the BIC operation, it is guaranteed that independently from the values of Q_s, Q_{set} and V_g, the current i_f is proven to remain bounded in the range described by inequality (18). However, the frequency ω should be guaranteed to remain bounded as well. By substituting (17) into (10) and consequently (10) to (12), the dynamics of ω become

$$\begin{aligned}
\dot{\omega} &= \frac{T_m}{J} - \frac{3(G_s+G)\omega M_f^2 i_f^2}{2J} + \frac{3M_f i_f V_g}{\sqrt{2}J}(G\cos\delta \\
&\quad + B\sin\delta) - \frac{D_p}{J}(\omega - \omega_r) \\
&= -\left(\frac{D_p}{J} + \frac{3(G_s+G)M_f^2 i_f^2}{2J}\right)\omega + \frac{T_m}{J} + \frac{D_p}{J}\omega_r \\
&\quad + \frac{3M_f i_f V_g}{\sqrt{2}J}(G\cos\delta + B\sin\delta) \\
&= -a\omega + v
\end{aligned} \tag{22}$$

where $a = \frac{D_p}{J} + \frac{3(G_s+G)M_f^2 i_f^2}{2J}$ and $v = \frac{T_m}{J} + \frac{D_p}{J}\omega_r + \frac{3M_f i_f V_g}{\sqrt{2}J}(G\cos\delta + B\sin\delta)$. Since it is guaranteed from the BIC operation that i_f verifies inequality (18) then

$$\frac{D_p}{J} + \frac{3(1-p)^2(G_s+G)V_n^2}{\omega_n^2} \leq a \leq \frac{D_p}{J} + \frac{3(1+p)^2(G_s+G)V_n^2}{\omega_n^2}, \tag{23}$$

with $D_p > 0$. Therefore a is always positive, i.e. $a \geq a_1$ with $a_1 = \frac{D_p}{J} + \frac{3(1-p)^2(G_s+G)V_n^2}{\omega_n^2}$. For the system (22), consider the Lyapunov function candidate

$$V = \frac{1}{2}\omega^2. \tag{24}$$

Then the time derivative of V becomes

$$\begin{aligned}
\dot{V} &= \omega\dot{\omega} = -a\omega^2 + \omega v \\
&\leq -a_1\omega^2 + \omega v \\
&= -(1-\beta)a_1\omega^2 - \beta a_1\omega^2 + \omega v \\
&\leq -(1-\beta)a_1\omega^2 \quad \forall\, |\omega| \geq \frac{|v|}{\beta a_1},
\end{aligned}$$

with $0 < \beta < 1$, which proves that system (22) is input-to-state stable (ISS) [14] by considering v as an input. Since i_f is bounded from the BIC operation and the variables V_g, T_m,

$$\begin{bmatrix} \dot{i}_f \\ \dot{i}_{fq} \end{bmatrix} = \begin{bmatrix} -k\left(\frac{(i_f - i_{fn})^2}{\Delta i_{fmax}^2} + i_{fq}^2 - 1\right) & i_{fq}\left(\frac{1}{KM_f}(Q_{set} - Q_s) + \frac{D_q}{KM_f}(V_n - V_g)\right) \\ -\frac{\epsilon^2 i_{fq}}{\Delta i_{fmax}^2}\left(\frac{1}{KM_f}(Q_{set} - Q_s) + \frac{D_q}{KM_f}(V_n - V_g)\right) & -k\left(\frac{(i_f - i_{fn})^2}{\Delta i_{fmax}^2} + i_{fq}^2 - 1\right) \end{bmatrix} \begin{bmatrix} i_f - i_{fn} \\ i_{fq} \end{bmatrix} \tag{20}$$

TABLE I
SYNCHRONVERTER PARAMETERS

Parameters	Values	Parameters	Values
L_s	$0.15mH$	L_g	$0.15mH$
R_s	0.045Ω	R_g	0.045Ω
C	$22\mu F$	nominal frequency	$50Hz$
R (parallel to C)	1000Ω	nominal phase voltage	$12Vrms$
rated power	$100VA$	DC-link voltage	$42V$

ω_g are bounded along with the sinusoidal signals $\sin\delta$ and $\cos\delta$, then v is a bounded signal too. As a result, it is guaranteed that the frequency ω of the synchronverter is always bounded from the ISS property of system (22). Therefore, E is proven to remain bounded from (17) which concludes the stability of the system in the sense of boundedness.

V. SIMULATION RESULTS

In order to investigate the proposed approach, the same scenario of the original synchronverter (SV) as illustrated in [1], [7] is considered and compared with the synchronverter operating with the BIC (SV+BIC), as proposed in the present paper. The synchronverter parameters are shown in Table I. It is assumed that a step-up transformer is used to connect the synchronverter with the grid and therefore the simulations are conducted with relatively low voltages.

A PLL is used for the initial synchronisation and therefore the first $0.5s$ doesn't play a significant role since during this period the SV is not connected to the grid. Initially $P_{set} = 0$ and $Q_{set} = 0$. At the time instant $t = 0.5s$, the circuit breaker is turned on and the SV is connected to the grid. At $t = 1s$, the real power reference becomes $P_{set} = 80W$, and at $t = 1.5s$, the reactive power reference is set to $Q_{set} = 60Var$. The droop control is enabled at $t = 2s$ and the grid voltage decreases by 5% at $t = 2.5s$. This scenario and the assumptions mentioned are taken from [7] to have a direct comparison. The performance of SV is compared to the SV+BIC with the same parameters $D_p = 0.2026$, $D_q = 117.88$, $K = 740.645$ and $J = 4.052\times10^{-4}$. The value of parameter M_f is not needed since it is combined with the field-excitation current as $M_f i_f$. For the SV+BIC, a maximum allowed field-excitation current deviation $\Delta i_{fmax} = 0.05 i_{fn}$ (5% above and below the rated value) and a maximum frequency deviation $\Delta f_{max} = 0.5Hz$ (1% of the rated frequency) are considered and the BIC gain k is chosen as $k = 1000$.

As it can be observed in Fig. 5, both the SV and the SV+BIC provide almost the same response since the BIC approximates the behaviour of the SV near the rated value. The SV is connected at $t = 0.5s$ and the frequency is synchronised at $50Hz$. The real and reactive power are also regulated to their values and the reactive power drops at $t = 2s$ since the droop controller is enabled. Finally, the SV is also regulated and remains stable even after the grid voltage drops by 5% at $t = 2.5s$, with the field excitation current i_f always remaining in the bounded range and verifying the theoretical analysis. The BIC operation for the field-excitation current dynamics is observed in Fig. 6, where it is verified that both controller states i_f, and i_{fq} travel exclusively on the ellipse W_0, staying within the given bounds at all times. As a result, by incorporating the BIC to the original SV, the same behaviour can be achieved in order to maintain the advantages of the SV and additionally guarantee non-linear stability in the sense of boundedness.

VI. CONCLUSIONS

In this paper, the non-linear stability in the sense of boundedness of the synchronverter connected to the grid was investigated and proven for the first time. After obtaining the complete non-linear dynamic model of the synchronverter, the field-excitation current loop was implemented using the BIC to produce a bounded output within a given range and to approximate the original synchronverter operation near the rated value. Taking into account this fact and using input-to-state stability theory, it was proven that the frequency dynamics will also remain bounded, thus resulting in a bounded synchornverter voltage which completes the closed-loop system stability in the sense of boundedness. Extensive simulation results comparing the original synchronverter and the synchronverter with the BIC suitably verify the proposed approach.

Although, the boundedness of the synchronverter was proven in the present paper, it is interesting to investigate the conditions required to prove the asymptotic convergence to a unique desired equilibrium. This will complete the stability analysis of the synchronverter and therefore provides an interesting topic for future research.

REFERENCES

[1] Q.-C. Zhong and T. Hornik, *Control of Power Inverters in Renewable Energy and Smart Grid Integration*. Wiley-IEEE Press, 2013.

[2] C. Sao and P. Lehn, "Autonomous load sharing of voltage source converters," *IEEE Trans. Power Del.*, vol. 20, no. 2, pp. 1009–1016, Apr. 2005.

[3] J. Vasquez, J. Guerrero, A. Luna, P. Rodriguez, and R. Teodorescu, "Adaptive droop control applied to voltage-source inverters operating in grid-connected and islanded modes," *IEEE Trans. Ind. Electron.*, vol. 56, no. 10, pp. 4088–4096, Oct. 2009.

[4] Q.-C. Zhong, "Robust droop controller for accurate proportional load sharing among inverters operated in parallel," *IEEE Trans. Ind. Electron.*, vol. 60, no. 4, pp. 1281–1290, Apr. 2013.

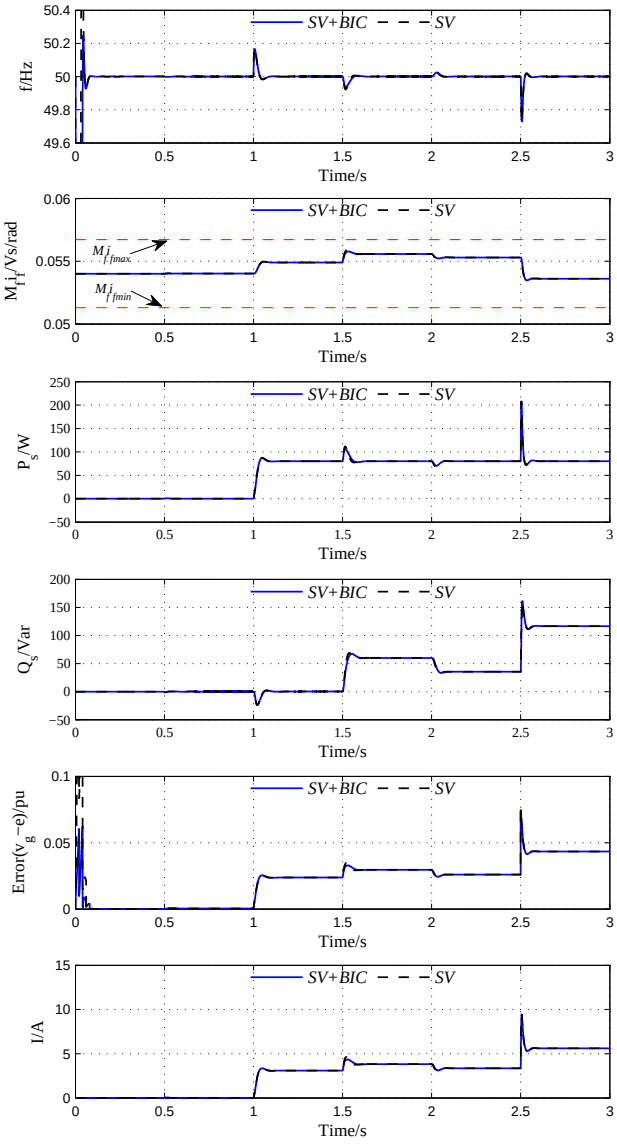

Fig. 5. Simulation results comparing the original synchronverter (SV) with the synchronverter operated with the BIC (SV+BIC)

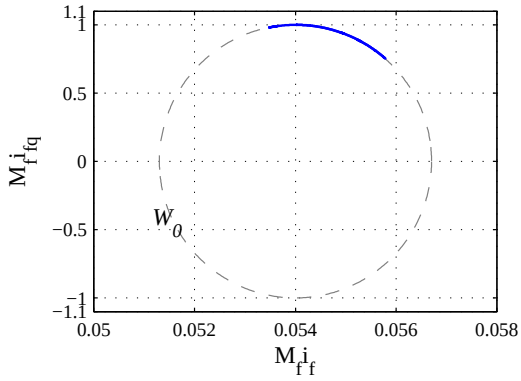

Fig. 6. Phase portrait of the BIC controller states

[5] J. Guerrero, M. Chandorkar, T. Lee, and P. Loh, "Advanced Control Architectures for Intelligent MicroGrids-Part I: Decentralized and Hierarchical Control," *IEEE Trans. Ind. Electron.*, vol. 60, no. 4, pp. 1254–1262, Apr. 2013.

[6] Y. Mohamed and E. El-Saadany, "Adaptive decentralized droop controller to preserve power sharing stability of paralleled inverters in distributed generation microgrids," *IEEE Trans. Power Electron.*, vol. 23, no. 6, pp. 2806–2816, Nov. 2008.

[7] Q.-C. Zhong and G. Weiss, "Synchronverters: Inverters that mimic synchronous generators," *IEEE Trans. Ind. Electron.*, vol. 58, no. 4, pp. 1259–1267, Apr. 2011.

[8] Q.-C. Zhong, P.-L. Nguyen, Z. Ma, and W. Sheng, "Self-synchronised Synchronverters: Inverters without a Dedicated Synchronisation Unit," *IEEE Trans. Power Electron.*, vol. 29, no. 2, pp. 617–630, Feb. 2014.

[9] Z. Ma, Q.-C. Zhong, and J. Yan, "Synchronverter-based Control Strategies for Three-phase PWM Rectifiers," in *Proc. of the 7th IEEE Conference on Industrial Electronics and Applications (ICIEA)*, Singapore, Jul. 2012.

[10] N. Pogaku, M. Prodanovic, and T. Green, "Modeling, Analysis and Testing of Autonomous Operation of an Inverter-Based Microgrid," *IEEE Trans. Power Electron.*, vol. 22, no. 2, pp. 613–625, 2007.

[11] M. Ashabani and Y. A.-R. I. Mohamed, "Integrating VSCs to Weak Grids by Nonlinear Power Damping Controller With Self-Synchronization Capability," *IEEE Trans. Power Syst.*, vol. 29, no. 2, pp. 805–814, 2014.

[12] P. S. Kundur, *Power System Stability and Control*. New York: McGraw-Hills, 1994.

[13] G. Konstantopoulos, Q.-C. Zhong, B. Ren, and M. Krstic, "Bounded Integral Control of Input-to-State Practically Stable Non-linear Systems to Guarantee System Stability and Achieve Fail-Safe Operation," 2014 (under review).

[14] H. K. Khalil, *Nonlinear Systems*. Prentice Hall, 2001.